The current issue and full text archive of this journal is available at
www.emeraldinsight.com/0961-5539.htm

Combined effects of the inlet temperature and the wall thermal capacitance on the laminar mixed convection in a vertical pipe

Received 28 November 2005
Revised 10 October 2006
Accepted 15 November 2006

Ton Hoang Mai and Catalin Viorel Popa
Laboratoire de Thermomécanique, UTAP, Faculté des Sciences, Reims, France, and
Omar Kholai
Laboratoire d'Energétique Appliquée et Pollution, Université de Constantine, Constantine, Algeria

Abstract

Purpose – The aim of this study is to present numerical analyses for combined effects of the inlet temperature (ΔT^+) and the wall-to-fluid thermal capacitance ratio (a^*) on the laminar mixed convection unsteady flows in a vertical pipe.

Design/methodology/approach – The full Navier-Stokes and energy, coupled, unsteady state, two-dimensional governing equations for ascending laminar mixed convection in a vertical pipe are solved numerically using a finite-difference scheme.

Findings – The results show that the thermohydraulic flow behaviour is highly dependent on both parameters (ΔT^+, a^*). Moreover, the unsteady characteristics of the flow can involve oscillatory and reversed flow phenomena yielding the unstable flows. For the heating case, the reversed flow appears below the wave instability and the unsteady vortex is always significant in the vicinity of the wall, whatever ΔT^+ and $a^* < 100$. For the cooling case, the reversed flow appears in the central region of the pipe; it develops on top of the wave instability.

Practical implications – This study should be very useful to improve heat transfer equipment.

Originality/value – The paper shows clearly the combined effects of both parameters (ΔT^+, a^*) on the laminar mixed convection flow.

Keywords Convection, Numerical analysis, Heat transfer, Flow

Paper type Research paper

Nomenclature

a^* = wall-to-fluid thermal capacitance ratio $((\rho C_p L)_w/(\rho C_p R)_f)$
C_p = heat capacity $\mathrm{J\,kg^{-1}K^{-1}}$
g = acceleration of the gravity ($\mathrm{ms^{-2}}$)
Gr = Grashof number ($g\beta\varphi_w R^4/v^2 k$)
k = thermal conductivity of the fluid ($\mathrm{W\,m^{-1}K^{-1}}$)
L = thickness of the wall
Pe = Peclet number ($Pr \cdot Re$)
Pr = Prandtl number (ν/α)
r = radial coordinate
R = radius of the pipe (m)
Re = Reynolds number ($V_d R/\nu$)
Ri = Richardson number (Gr/Re^2)
t = time (s)
T = temperature (°C)
U = velocity in the r-direction ($\mathrm{m\,s^{-1}}$)
V = velocity in the z-direction ($\mathrm{m\,s^{-1}}$)

International Journal of Numerical Methods for Heat & Fluid Flow
Vol. 18 No. 1, 2008
pp. 83-101

0961-5539
DOI 10.1108/09615530810839769

V_d = bulk velocity ($m\,s^{-1}$)
z = axial coordinate

Greek symbols
α = thermal diffusivity ($m^2\,s^{-1}$)
β = coefficient of thermal expansion (K^{-1})
ρ = fluid density ($kg\,m^{-3}$)
ΔT = temperature step (°C)
μ = dynamic viscosity ($kg\,m^{-1}\,s^{-1}$)
ν = kinematic viscosity ($m^2\,s^{-1}$)
ϕ = heat flux ($W\,m^{-2}$)
ψ = stream function ($m^3\,s^{-1}$)
Ω = vorticity (s^{-1})

Subscripts
a = ambient reference quantity
e = inlet
f = fluid
w = at the wall

Introduction

Unsteady mixed convection in ducts is an important branch of heat transfer research and technology. This phenomenon has many diverse industrial and engineering applications, such as nuclear plants, heat exchangers and other apparatuses, etc. In thermal equipments, transients may also rise due to changes in the operating conditions such as time-varying inlet temperature or flow rates. Unsteady characteristics of the flow in heat exchange equipments can involve in oscillatory and reversed flow phenomena yielding the unstable flows. These phenomena can also produce a reduction of the thermal system effectiveness and the severe thermal stress with eventual mechanical failure. Thus, it is important to know and predict the transient response of a heat exchanger for time-varying inlet temperature; it is also essential to know its transient response in order to provide an effective control system. The fundamental studies of unsteady convective heat transfer process have been presented by Kakac and Yener (1995) in their recent book. In the field of channel flows, the combined effects between free and forced convection through vertical tubes have been investigated numerically and experimentally by several researchers. Numerical analyses were performed by Cheng *et al.* (1990) and Hamadah and Wirtz (1991) with the establishment of the recirculating flow criteria for aiding and opposing mixed convection in vertical channel flows. Morton *et al.* (1989) focused their attention on a recirculating behaviour produced in mixed convection flows and compared the numerical results with experimental ones for water. Gau *et al.* (1992) and Huang *et al.* (1995) have experimentally studied the reversed flow structure and heat transfer in a finite asymmetrically heated vertical channel. The flow oscillation induced by the reversed flow has already been visualized (Bernier and Baliga, 1992a, b; Joye and Wojnovich, 1996). Wang *et al.* (1994) and Nesreddine *et al.* (1998) have studied the effects of the axial diffusion on the laminar mixed convection flows with low-Peclet numbers in the entrance region of thin vertical and horizontal tubes. These studies show that the axial diffusion plays a significant role in the fluid upstream preheating from the entrance of the heat transfer region and can lead to reversal flow. Similar studies (Heggs *et al.*, 1990; Zghal *et al.* 2001; Behzamehr *et al.*, 2003) also show the significance of the heat conduction effects in the wall on the development of the recirculating flow especially for low-Reynolds numbers. Barletta (2001) observed the reversal flow for laminar mixed convection in vertical channel with isothermal and isoflux boundary conditions. He showed that this phenomenon strongly depended on the friction factor and the sign of the Gr/Re parameter. A recent study on the aiding or the opposing mixed convection flows in a heating vertical pipe has been investigated

by Nguyen *et al.* (2004). The authors show the apparition of the recirculating flow in the wall vicinity for the aiding flow case and in the central region for the opposing flow case.

The investigations mentioned above are concerned with mixed convection through vertical or horizontal tubes, when a sudden change in the wall temperature or the wall heat flux occurs. There have been few investigations of inlet temperature variation which are used in practice as heat transfer media in the nuclear-reactor, cooling process and compact heat exchangers. This boundary condition plays a pronounced role in flow and heat transfer characteristics, as is well known for pure forced convection in pipes (Kakac *et al.*, 1990). In the mixed convection case in pipes, Mai *et al.* (2005) performed a numerical study to investigate the transient mixed convection flows in vertical tube subjected to a variation of the inlet temperature, when external convection has not a negligible effect any more. They show that the interaction between the hot and the cold fluids leads to the oscillation of the streamline and consequently to the laminar flow instability. In practice, laminar flow through vertical pipe will always be unstable, when the inlet boundary conditions are changing with time.

In the present study, the transient mixed convection flow instabilities in a vertical pipe are systematically analysed in view of the simultaneous effects of inlet temperature step and wall thermal capacitance. The full Navier-Stokes equations are used in our model. The variation of streamline and isotherm in the pipe are extensively investigated and the time development of the recirculating flow occurrence is clearly identified with the relevant flow parameters.

Problem formulation

We use a transient laminar mixed convection inside a vertical pipe with fully developed flow, which is subjected to a sudden variation of the inlet temperature. In practice applications, the inlet temperature of the heat exchanger may vary as a function of time. This condition is a valuable contribution to the industrially significant problem area of transient response of thermal systems. A general boundary condition of the fifth kind that take into account both heat flux through wall-fluid interface and wall heat capacitance effects is employed, while axial conduction effect is disregarded because the wall is considered to be very thin (Bernier and Baliga, 1992a, b; Nesreddine *et al.*, 1998). The geometry for the theoretical analysis is shown in Figure 1. The thermophysical properties of the fluid are supposed to be constant except in the buoyancy term (the Boussinesq approximation). The equations considered are the two-dimensional incompressible continuity, momentum, and energy equations in axial-symmetric coordinates. The governing equations are formulated in terms of the stream function and the vorticity defined as:

$$U^+ = -\frac{1}{r^+}\frac{\partial \Psi^+}{\partial z^+}; \quad V^+ = \frac{1}{r^+}\frac{\partial \Psi^+}{\partial r^+} \tag{1}$$

$$\Omega^+ = \frac{\partial U^+}{\partial z^+} - \frac{\partial V^+}{\partial r^+} \tag{2}$$

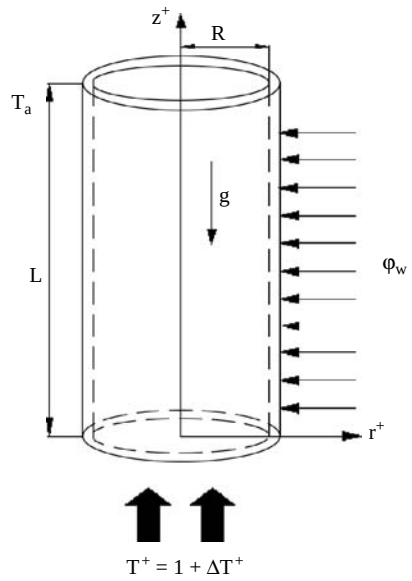

Figure 1.
Schematic diagram of the physical model

The non-dimensional momentum, energy and Poisson equations are:

$$\frac{\partial \Omega^+}{\partial t^+} + \frac{\partial (\Omega^+ V^+)}{\partial z^+} + \frac{\partial (\Omega^+ U^+)}{\partial r^+} = \frac{1}{Re}\left[\frac{1}{r^+}\frac{\partial}{\partial r^+}\left(r^+ \frac{\partial \Omega^+}{\partial r^+}\right) + \frac{\partial^2 \Omega^+}{\partial z^{+2}}\right] - Ri\frac{\partial T^+}{\partial r^+} \quad (3)$$

$$\frac{\partial T^+}{\partial t^+} + \frac{1}{r^+}\frac{\partial (r^+ U^+ T^+)}{\partial r^+} + \frac{\partial (V^+ T^+)}{\partial z^+} = \frac{1}{Pe}\left[\frac{1}{r^+}\frac{\partial}{\partial r^+}\left(r^+ \frac{\partial T^+}{\partial r^+}\right) + \frac{\partial^2 T^+}{\partial z^{+2}}\right] \quad (4)$$

$$-\Omega^+ = \frac{\partial}{\partial r^+}\left(\frac{1}{r^+}\frac{\partial \Psi^+}{\partial r^+}\right) + \frac{1}{r^+}\frac{\partial^2 \Psi^+}{\partial z^{+2}} \quad (5)$$

where the following dimensionless quantities are:

$$r^+ = \frac{r}{R}; \quad z^+ = \frac{z}{R}; \quad U^+ = \frac{U}{V_d}; \quad V^+ = \frac{V}{V_d}; \quad T^+ = \frac{\lambda_f}{\varphi_w R}(T - T_a);$$

$$t^+ = \frac{V_d}{R}t; \quad \Omega^+ = \frac{R}{V_d}\Omega; \quad \Psi^+ = \frac{1}{V_d R^2}\Psi$$

Equations (1)-(5) are subject to specific initial and boundary conditions. The initial conditions are:

$$-t^+ = 0, \quad 0 \le r^+ \le 1, \quad \forall z^+ : V^+ = 2(1 - r^{+2}); \quad T^+ = 1$$

The boundary conditions for $t^+ > 0$ are:

$$-z^+ = 0 : \Psi^+ = r^{+^2}\left(1 - \frac{r^{+^2}}{2}\right) - \frac{1}{2}; \quad \Omega^+ = 4r^+; \quad T^+ = 1 + \Delta T^+$$

where:

$$\Delta T^+ = \frac{\lambda_f}{\varphi_w R}\Delta T \quad (\Delta T^+ > 0 \text{ or } < 0 \quad) - r^+ = 0 : \frac{\partial T^+}{\partial r^+} = 0;$$

$$\Psi^+ = \text{arbitrary constant}; \quad \Omega^+ = 0 \quad - r^+ = 1 : \Psi^+ = 0$$

On the pipe wall, the fifth kind of boundary condition (Kakac *et al.*, 1990) is imposed as:

$$\rho C_p L \frac{\partial T}{\partial t} = -\varphi_{wi} + \varphi_w$$

where ϕ_{wi} is the heat flux through wall-fluid interface and ϕ_w is the wall heat flux.

The dimensionless wall heat flux (Φ_w)which is used to describe energy transfer into the fluid through the wall-fluid interface is evaluated as:

$$\Phi_w = \frac{\varphi_{wi}}{\varphi_w} = \left(\frac{\partial T^+}{\partial r^+}\right)_w = 1 - a^* Pr \frac{\partial T^+}{\partial t^+}$$

where:

$$(a^* = (\rho C_p L)_w/(\rho C_p R)_f)$$

is the wall-to-fluid thermal capacitance ratio.

Numerical method

The solution for the problem defined by the foregoing equations is solved by finite-difference procedures. An implicit numerical scheme is used for Poisson equation and an explicit numerical scheme is employed for the momentum and energy equations, in which forward differencing is used in time and central differencing on the linear spatial terms. To preserve the stability of the numerical scheme the non-linear spatial terms:

$$(\partial(V^+T^+)/\partial z^+, \partial(r^+U^+T^+)/\partial r^+, \partial(V^+\Omega^+)/\partial z^+ \text{ and } \partial(U^+\Omega^+)/\partial r^+)$$

are approximated with special non-central differences described by Torrance and Rockett (1969). The special forms are:

$$\left(\frac{\partial(V^+f)}{\partial z^+}\right)_{ij} = \frac{1}{\Delta z^+}\left(\frac{V^+_{i+1,j} + V^+_{ij}}{2} f_{ij} - \frac{V^+_{ij} + V^+_{i-1,j}}{2} f_{i-1,j}\right) \tag{6a}$$

when the coefficients $1/2(V^+_{i+1,j} + V^+_{ij})$ and $1/2(V^+_{ij} + V^+_{i-1,j})$ are positive:

$$\left(\frac{\partial(V^{+}f)}{\partial z^{+}}\right)_{ij}=\frac{1}{\Delta z^{+}}\left(\frac{V^{+}_{i+1,j}+V^{+}_{ij}}{2}f_{i+1,j}-\frac{V^{+}_{ij}+V^{+}_{i-1,j}}{2}f_{ij}\right) \tag{6b}$$

when the coefficients are negative.

The variable f represents either T^{+}or $\Omega^{+}$and the subscripts denote the spatial location of grid points. When the coefficients are of a different sign, a mixed expression is required which contains one term from each of the equations (6), as appropriate. A similar procedure is used to approximate $\partial(r^{+}U^{+}T^{+})/\partial r^{+}$ and $\partial(U^{+}\Omega^{+})/\partial r^{+}$ according to the sign of $1/2\left(U^{+}_{i,j+1}+U^{+}_{ij}\right)$ and $1/2\left(U^{+}_{ij}+U^{+}_{i,j-1}\right)$.

The product of the variable f in equations (6) represents a convective transport of f between node points $(i+1,j)$ and (i,j) or (i,j) and $(i-1,j)$. For example, the selection of f_{ij} or $f_{i+1,j}$ is necessary for f to be strictly conserved in the transport between the nodes according to the sign of the mean velocity.

In the case where the non-linear derivatives are represented by forms similar to the equation (6a), the discretized equations (3) and (4) can be written:

$$\begin{aligned}&\frac{\Omega^{+^{n+1}}_{ij}-\Omega^{+^{n}}_{ij}}{\Delta t^{+}}+\frac{\left(V^{+^{n}}_{i+1,j}+V^{+^{n}}_{ij}\right)\Omega^{+^{n}}_{ij}-\left(V^{+^{n}}_{ij}+V^{+^{n}}_{i-1,j}\right)\Omega^{+^{n}}_{i-1,j}}{2\Delta z^{+}}\\&\quad+\frac{\left(U^{+^{n}}_{i,j-1}+U^{+^{n}}_{ij}\right)\Omega^{+^{n}}_{ij}-\left(U^{+^{n}}_{ij}+U^{+^{n}}_{i,j-1}\right)\Omega^{+^{n}}_{i,j-1}}{2\Delta r^{+}}\\&=-Ri\frac{T^{+^{n+1}}_{i,j+1}-T^{+^{n+1}}_{i,j-1}}{2\Delta r^{+}}+\frac{1}{Re}\frac{\Omega^{+^{n}}_{i+1,j}-2\Omega^{+^{n}}_{ij}+\Omega^{+^{n}}_{i-1,j}}{\Delta z^{+^{2}}}\\&\frac{1}{Re}\frac{\left[(j+1)/(j+1/2)\right]\Omega^{+^{n}}_{i,j+1}-\left[j/(j+1/2)+j/(j-1/2)\right]\Omega^{+^{n}}_{ij}+\left[(j+1)/(j-1/2)\right]\Omega^{+^{n}}_{i,j-1}}{\Delta r^{+^{2}}}\end{aligned} \tag{7}$$

$$\begin{aligned}&\frac{T^{+^{n+1}}_{ij}-T^{+^{n}}_{ij}}{\Delta t^{+}}+\frac{\left(V^{+^{n}}_{i+1,j}+V^{+^{n}}_{ij}\right)T^{+^{n}}_{ij}-\left(V^{+^{n}}_{ij}+V^{+^{n}}_{i-1,j}\right)T^{+^{n}}_{i-1,j}}{2\Delta z^{+}}\\&\quad+\frac{(j+1/2)\left(U^{+^{n}}_{i,j+1}+U^{+^{n}}_{ij}\right)T^{+^{n}}_{ij}-(j-1/2)\left(U^{+^{n}}_{ij}+U^{+^{n}}_{i,j-1}\right)T^{+^{n}}_{i,j-1}}{2j\Delta r^{+}}\\&=\frac{1}{Pe}\left[\frac{(j+1/2)T^{+^{n}}_{i,j+1}-2jT^{+^{n}}_{ij}+(j-1/2)T^{+^{n}}_{i,j-1}}{j\Delta r^{+^{2}}}+\frac{T^{+^{n}}_{i+1,j}-2T^{+^{n}}_{ij}+T^{+^{n}}_{i-1,j}}{\Delta z^{+^{2}}}\right]\end{aligned} \tag{8}$$

At the centreline, a special form of the equation (8) is used which incorporates boundary conditions:

$$\frac{T_{i,o}^{+^{n+1}} - T_{i,o}^{+^n}}{\Delta t^+} + \frac{\left(V_{i+1,o}^{+^n} - V_{i,o}^{+^n}\right) T_{i,o}^{+^n} - \left(V_{i,o}^{+^n} - V_{i-1,o}^{+^n}\right) T_{i-1,o}^{+^n}}{2\Delta z^+} + 2T_{i,o}^{+^n} \frac{U_{i,1}^{+^n}}{\Delta r^+}$$
$$= \frac{1}{Pe}\left[4\frac{T_{i,1}^{+^n} - T_{i,o}^{+^n}}{\Delta r^{+^2}} + \frac{T_{i+1,o}^{+^n} - 2T_{i,o}^{+^n} + T_{i-1,o}^{+^n}}{\Delta z^{+^2}}\right] \quad (9)$$

Equations (7)-(9) thus allows $\Omega_{ij}^{+^{n+1}}$ and $T_{ij}^{+^{n+1}}$ at all interior grid points to be explicitly calculated at the moment $n + 1$ according to the known quantities at the moment n.

From equations (7) to (9), we have obtained the following system of equations:

$$T_{ij}^{+^{n+1}} = a_1 T_{i+1,j}^{+^n} + a_2 T_{i-1,j}^{+^n} + a_3 T_{ij}^{+^n} + a_4 T_{i,j+1}^{+^n} + a_5 T_{i,j-1}^{+^n} \quad (10)$$

$$\Omega_{ij}^{+^{n+1}} = b_1 \Omega_{i+1,j}^{+^n} + b_2 \Omega_{i-1,j}^{+^n} + b_3 \Omega_{ij}^{+^n} + b_4 \Omega_{i,j+1}^{+^n} + b_5 \Omega_{i,j-1}^{+^n} + c \quad (11)$$

where a_k, b_k ($k = 1,2, \ldots 5$) and c are algebraical coefficients which are constant over a time step.

The scheme stability in the sense of Lax and Richtmyer (1956) is obtained if all the coefficients a_k and b_k are positive. The coefficients a_k, b_k ($k = 1, 2, 4, 5$) in equations (10)-(11) are always positive, whereas a_3 and b_3 can be made positive by restricting the size of the time step Δt^+.

Concerning the stability criterion of numerical scheme, the time step Δt^+ is determined according to the sign of mean velocities (U^+ or V^+). For example, if a_3, $b_3 \geq 0$ and if approximations similar to equation (6a) are used, the vorticity equation provides the greatest restriction on Δt^+. Equation (7) requires that:

$$\Delta t^+ \leq \left[\frac{j/(j+1/2) + j/(j-1/2)}{Re\,\Delta r^{+^2}} + \frac{2}{Re\,\Delta z^{+^2}} + \frac{U_{i,j+1}^{+^n} + U_{ij}^{+^n}}{2\Delta r^+} + \frac{V_{i+1,j}^{+^n} + V_{ij}^{+^n}}{2\Delta z^+}\right]^{-1} \quad (12)$$

whereas equation (8) requires:

$$\Delta t^+ \leq \left[\frac{2}{Pe\Delta z^{+^2}} + \frac{2}{Pe\Delta r^{+^2}} + \frac{(j+1/2)\left(U_{i,j+1}^{+^n} + U_{ij}^{+^n}\right)}{2j\Delta r^+} + \frac{V_{i+1,j}^{+^n} + V_{ij}^{+^n}}{2\Delta z^+}\right]^{-1} \quad (13)$$

and equation (9) requires:

$$\Delta t^+ \leq \left[\frac{2}{Pe\Delta z^{+^2}} + \frac{4}{Pe\Delta r^{+^2}} + \frac{2U_{i,1}^{+^n}}{\Delta r^+} + \frac{V_{i+1,o}^{+^n} + V_{i,o}^{+^n}}{2\Delta z^+}\right]^{-1} \quad (14)$$

Additional forms similar to equations (12)-(14) arise when the alternative approximations (6b) are used.

The field of mesh points is scanned in order to determine the largest permissible Δt^+ which will satisfy the stability requirements on the whole equation

described previously. Moreover, we have used in this study a grid spacing of $\Delta z^+ = 0.1$ and $\Delta r^+ = 0.025$, with a total of 32,841 mesh points.

The new vorticities $\Omega_{ij}^{+^{n+1}}$ are next introduced into the stream function equation, which is solved for the new stream function field by the method of successive over-relaxation (Bejan, 1984). These new values are calculated by an iterative procedure. After m iterations, a further approximation $\Psi_{ij}^{+^{m+1}}$ is obtained from:

$$\Psi_{i,j}^{+^{m+1}} = (1-\omega)\Psi_{i,j}^{+^{m}} + \left[\frac{\omega}{\frac{2}{(\Delta z^+)^2} + \frac{1}{(\Delta r^+)^2}\left(\frac{j}{j+(1/2)} + \frac{j}{j-(1/2)}\right)}\right] \left[j(\Delta r^+)\Omega_{i,j}^{+^{n+1}} + \frac{1}{(\Delta z^+)^2}\left(\Psi_{i+1,j}^{+^{m}} + \Psi_{i-1,j}^{+^{m+1}}\right) + \frac{1}{(\Delta r^+)^2}\left(\frac{j}{j+(1/2)}\Psi_{i,j+1}^{+^{m}} + \frac{j}{j-(1/2)}\Psi_{i,j-1}^{+^{m+1}}\right)\right] \tag{15}$$

The relaxation parameter ω is chosen equal to 1.9 giving a good convergence of the numerical scheme.

The new wall vorticities are then calculated from the stream function field in the vicinity of the wall, using a Taylor series expansions for Ψ^+ near the wall.

Finally, new fields of U^+ and V^+ are obtained from three-point central difference approximations applied to the velocity equations. The fields of Ω^+, T^+, Ψ^+, U^+ and V^+ are thus made current at time level $t^+ = t^+ + \Delta t^+$.

Once the transient solution died out, the temperature and velocity fields are integrated over a sufficiently long period of time for the steady components of the respective field variables to be evaluated. These variables that are averaged in time are used to evaluate axial distributions of the local Stanton number and the local friction factor. The Stanton numbers and the friction factors are evaluated using the following definitions:

$$St = \frac{\varphi_w}{\rho C_p V_d (T_e - T_w)}; \quad C_f = \frac{-\mu(\partial V/\partial r)_{r=R}}{(1/2)\rho V_d^2}$$

The numerical scheme has been successfully validated by comparing calculated results with available data from literature. Figure 2 shows a comparison of the calculated axial velocity with the corresponding results calculated by Zghal *et al.* (2001) for upward flow of air in a heated isothermal vertical tube. One can notice a very good agreement between both models.

Results

In the present study, the following conditions are selected in the computations: water flow, copper pipe of diameter 20/22 mm. In the initial state, the temperature of the fluid is uniform and the flow is fully developed (parabolic profile). The uniform heat flux is imposed on the external surface of the pipe. A positive or negative temperature step is suddenly applied to the entrance of the pipe. Numerical results are obtained for ΔT^+ ranging from -0.73 to $+0.73$, a^* ranging from 40 to 100, the Reynolds number ranging from 100 to 600 and the Grashof number ranging from 2×10^5 to 7×10^5.

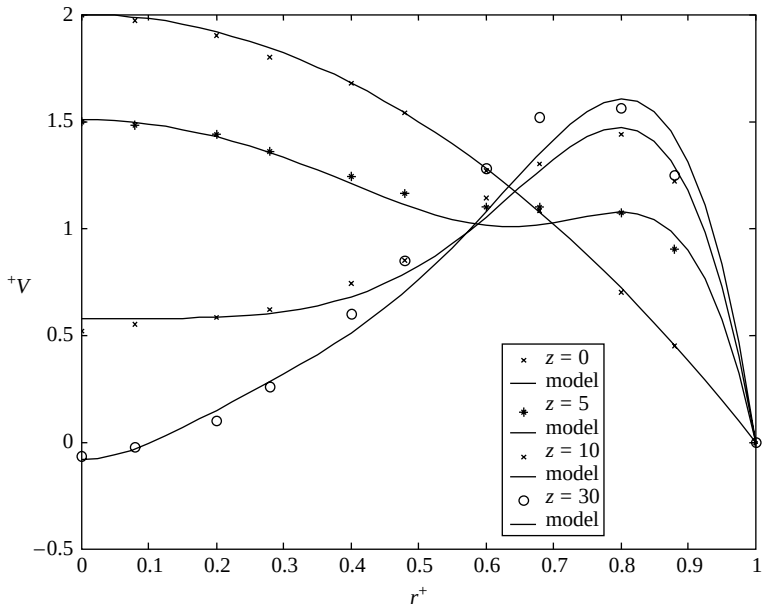

Notes: Between the model and the available data from the literature for Re = 500, Ri = 4, Pr = 0.7 and different sections

Figure 2.
Comparison of the axial velocity profiles

In the heating process case ($\Delta T^{+} > 0$), after a sudden perturbation at the pipe entrance and under the buoyancy effect, the fluid velocity is increasing along the centreline due to heating and is decreasing near the wall in order to satisfy the global mass conservation. This causes a distortion in the velocity profile (Figure 3(a)). In this case, the distortion is maximal at 15 s. On the other hand, the reduction of the streamwise velocity near the wall can lead to a reversal flow, consequently the distortion of the thermal field, as it can be shown in the Figure 3(b). A highly distorted fluid temperature induced by a high-reversal flow near the wall leads to two local minima, one observed near the centreline due to the heating of the fluid in the central region of the pipe and the other one located in the near wall region. The second is due to the presence of a recirculation zone near the wall, as we may observe later on the corresponding streamlines. This phenomenon has also been observed by Nguyen *et al.* (2004). It is also observed that the radial temperature gradient has considerably increased on the wall pipe, indicating that heat transfer has obviously become more important at this axial location.

The time development of streamlines and isotherms along the pipe for $\Delta T^{+} = +0.15$, $a^{*} = 70$ and $Re = 100$, are shown on the Figure 4. Under the simultaneous effects of the inlet temperature step and the wall thermal capacitance, a vortex begins to form in the vicinity of the wall at 5 s. As time increases, the vortices eventually dissipate near the wall and propagate along the wall. The apparition of co-rotative vortices below the wave instability leads to a reversal flow near the wall, in other words an oscillatory-like flow behaviour, therefore unstable. Figure 5 shows the effects of the inlet temperature step on the thermohydraulic flow behaviour.

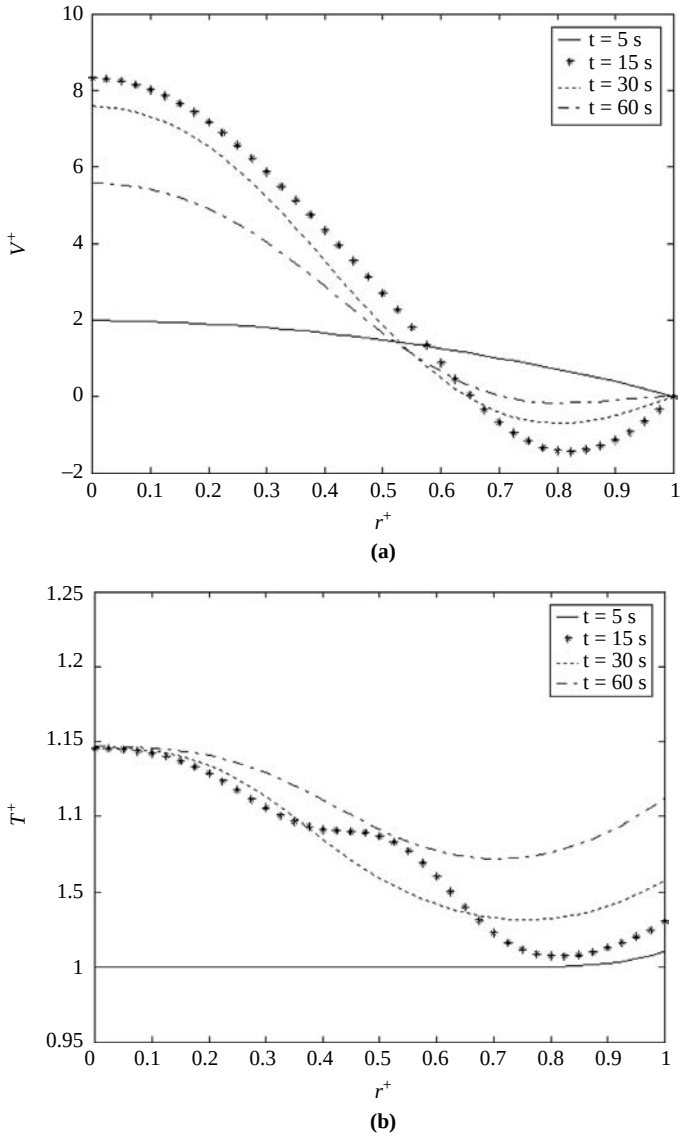

Figure 3.
(a) Velocity profiles for $z^+ = 20$, $Re = 100$, $\Delta T^+ = 0.15$ and $Gr = 2 \times 10^5$; (b) temperature profiles for $z^+ = 20$, $Re = 100$, $\Delta T^+ = 0.15$ and $Gr = 2 \times 10^5$

The formation of vortex instability appears for $\Delta T^+ = +0.15$. When ΔT^+ is higher than $+0.37$, a secondary vortex appears in the vicinity of the wall. The oscillation of the flow induced by vortices also leads to the wall boundary layer instability. This phenomenon is due to the interaction between hot and cold fluid. Like flow fluctuations, thermal perturbations are also active at the interface between the boundary layer along the wall and the central region of the pipe.

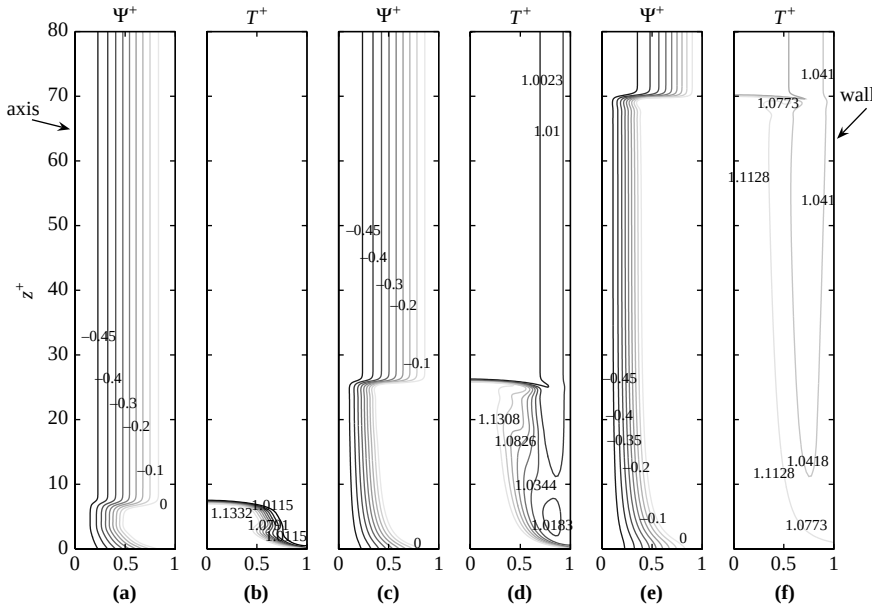

Notes: For Re = 100, ΔT^{+} = 0.15, $Gr = 2 \times 10^{5}$; (a) and (b) 5 s, (c) and (d) 15 s, (e) and (f) 40 s

Figure 4.
Time development of streamlines and isotherms

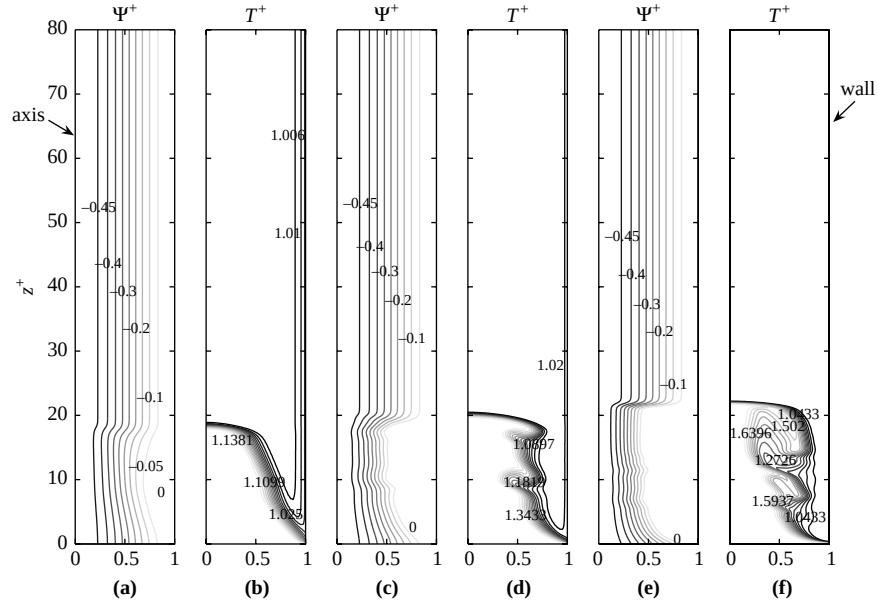

Notes: For t = 5s, Re = 300, $Gr = 2 \times 10^{5}$ and different ΔT^{+}; (a) and (b) 0.15, (c) and (d) 0.37, (e) and (f) 0.73

Figure 5.
Streamlines and isotherms along the pipe

It is interesting to analyse the thermohydraulic flow behaviour under the combined effects of the inlet temperature and the wall-to-fluid thermal capacitance ratio. The streamlines and isotherms along the pipe for $Re = 300$, $Gr = 7 \times 10^5$, $\Delta T^+ = +0.04$ and a^* ranging from 40 to 100, are shown in the Figure 6. For the low a^* ($a^* = 40$), the flow is accelerated in the central region. The flow acceleration leads to the reduction of the streamwise velocity near the wall and consequently to the recirculation zone in the vicinity of the wall. The fluid temperature at the centreline is hotter than the one near the wall and it decreases when a^* increases ($a^* = 70$). The isotherms present a minimum near the wall due to the reversal flow and the oscillation of the flow. The flow behaviour changes when a^* value becomes significant ($a^* = 100$). Contrary to the previous case, the flow is increasing near the wall and is decreasing in the centre of the pipe. The decreasing of the flow in the central region leads to the recirculation zone. Moreover, the secondary recirculation zone appears at the interface between the boundary layer and the central region due to the interaction between the hot fluid near the wall and the cold fluid in the central region; consequently, a thermal field instability develops at the pipe exit.

Let us consider now the cooling process ($\Delta T^+ < 0$) for $\Delta T^+ = -0.73$, $a^* = 70$ and $Re = 100$ (Figure 7). Contrary to the case for a positive temperature step, under the thermal capacitance effect, the flow is accelerated near the wall and decreases near the centreline; consequently a reversal flow develops (Figure 7(a)). The effects due to the reversal flow on the fluid temperature profiles may be shown in Figure 7(b) for the same axial location considered. The heating effect obviously becomes more pronounced especially in the wall vicinity where the radial temperature gradient has considerably increased. During the transient phase, streamlines and isotherms oscillate in time and propagate along the pipe (Figure 8). In this case, the reversal flow appears about 60 s and on top of the wave instability. The thermal capacitance effect is dominant in comparison with the inlet temperature step. Streamline and isotherm evolutions along the pipe for different $\Delta T^+ < 0$ are shown in Figure 9. Whatever the negative temperature step, the reversal flow appears near the centreline. For the low-temperature step ($\Delta T^+ = -0.15$), the deceleration of the flow at the centreline due to the wall thermal capacitance leads to the recirculation zone therefore the flow becomes unstable.

Figure 10 shows the streamline and isotherm evolutions along the pipe for different a^*. The flow oscillates along the pipe for a low a^* value ($a^* = 40$) and the flow becomes highly unstable when the a^* value increases. The reversal flow development appears near the entrance region for a high a^* value ($a^* = 100$); consequently the fluid temperature increases near the wall. This result shows that the laminar mixed convection flow behaviour is highly dependent on the wall thermal capacitance effect.

The combined effects of the inlet temperature and the wall thermal capacitance lead to laminar flow instabilities; consequently to the heat transfer of the fluid. In Figures 11 and 12, local values of the Stanton number and the friction factor are plotted versus the non-dimensional axial distance from the entrance region, for different positive temperature steps, $Re = 600$ and $a^* = 70$. The Stanton number rapidly decreases and presents a local minimum near the entrance region when the temperature steps increase ($\Delta T^+ > 0.15$). This is due to the presence of the recirculating flow as it is shown in Figure 4. Contrary to the Stanton number, the friction factor decreases with

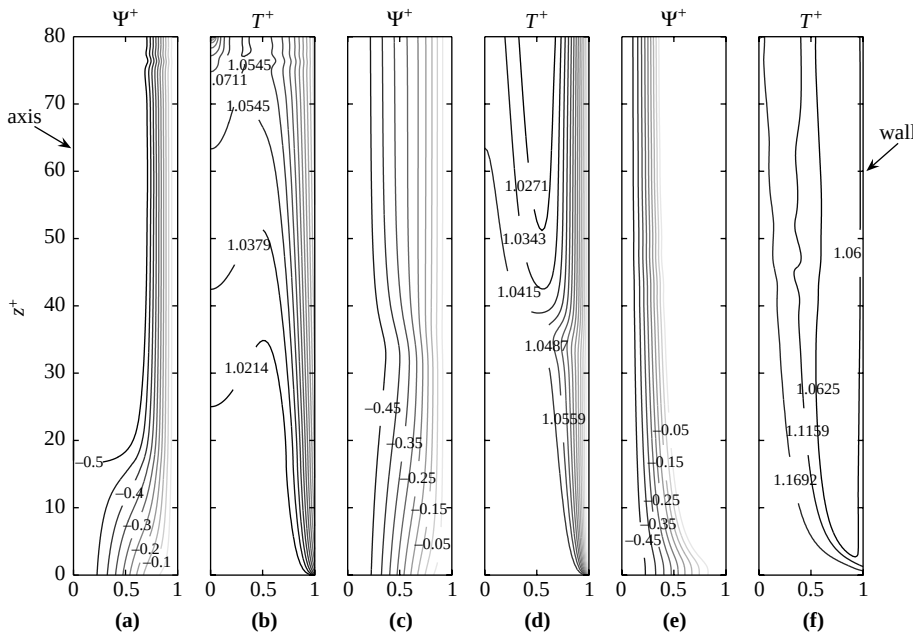

Notes: For t = 30 s, Re = 300, ΔT^+ = +0.04, Gr = 7×10^5 and different a*; (a) and (b) 100, (c) and (d) 70, (e) and (f) 40

Figure 6.
Streamlines and isotherms along the pipe

the increasing of the axial distance in the pipe. However, the existence of the recirculating flow near the wall can lead to negative friction factor values.

In the cooling process case (Figures 13 and 14), both parameters the Stanton number and the friction factor grow with the increasing of the temperature steps. The local values of the Stanton number slightly decrease with the increasing of the axial distance. The friction factor increases as a function of the axial distance. This is due to the flow acceleration near the wall.

For all studied cases, the results show that the heat transfer and the friction factor are depending not only on both parameters (ΔT^+, a^*) but also on the axial distance in the pipe.

Conclusion

The effects of the temperature step and the wall-to-fluid thermal capacitance ratio on the mixed convection flows in the vertical pipe are investigated numerically. The interaction between the hot and the cold fluids leads to laminar mixed convection flow instabilities.

In the heating process case, the reversal flow appears below the wave instability and the unsteady vortex is always significant in the vicinity of the wall whatever the temperature step and for low a^* values ($a^* < 100$). On the other hand, the reversal flow appears in the central region for high a^* values ($a^* \geq 100$). The Stanton number rapidly decreases with the increasing of the axial distance and takes a local minimum

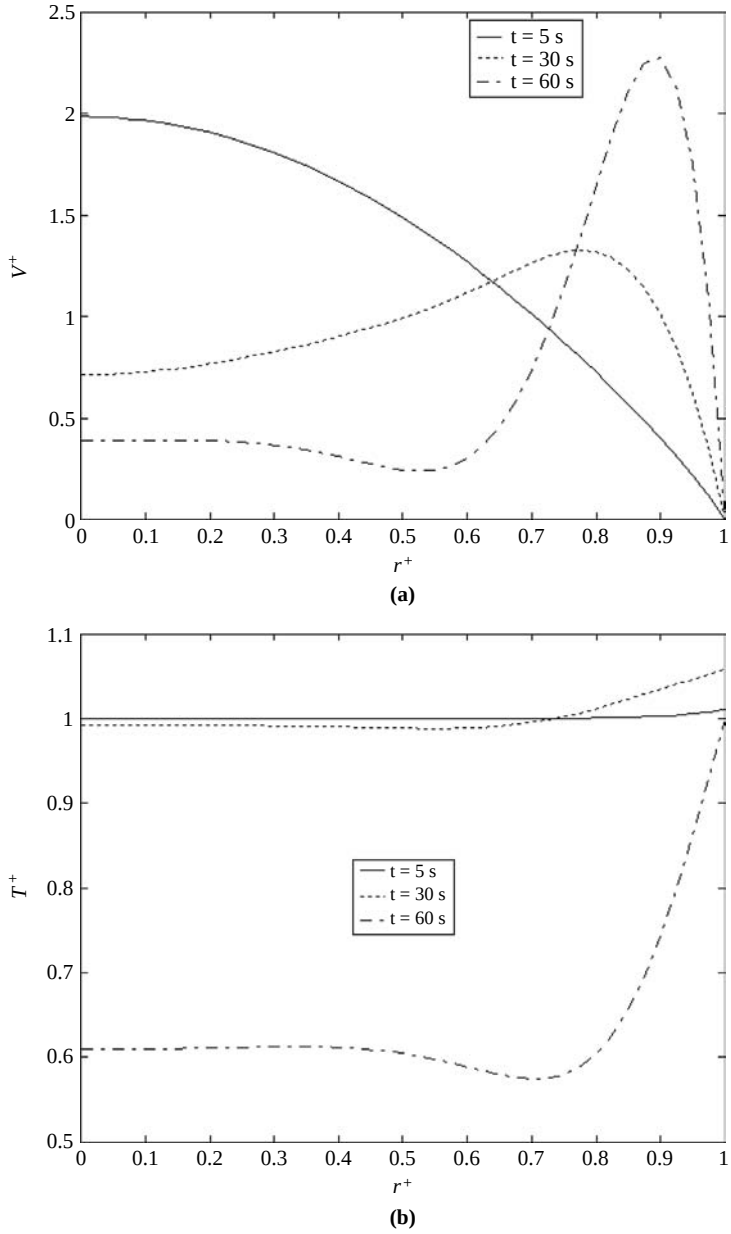

Figure 7.
(a) Velocity profiles for $z^+ = 20$, $Re = 100$, $Gr = 2 \times 10^5$ and $\Delta T^+ = -0.73$; (b) temperature profiles for $z^+ = 20$, $Re = 100$, $Gr = 2 \times 10^5$ and $\Delta T^+ = -0.73$

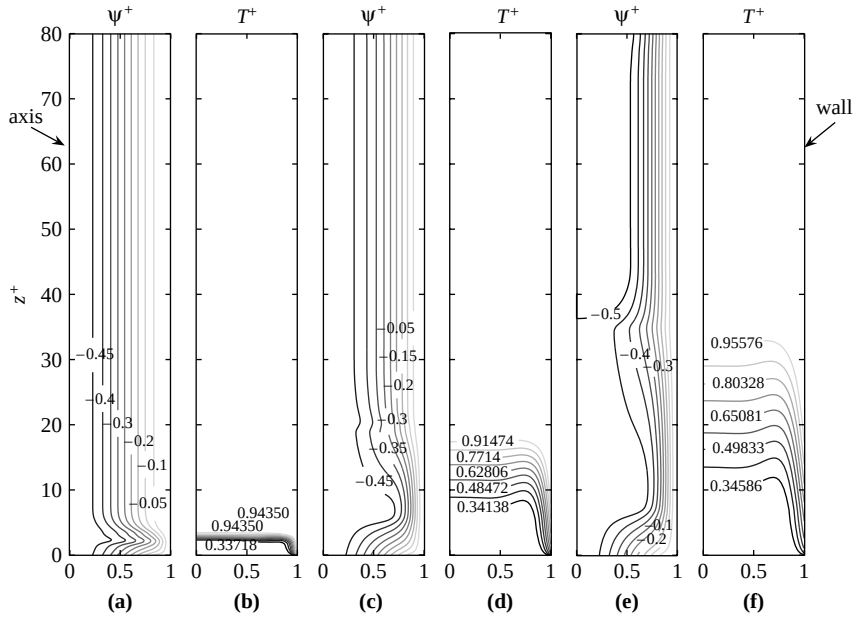

Figure 8.
Time development of streamlines and isotherms

Notes: For $Re = 100$, $\Delta T^{+} = -0.73$, $Gr = 2 \times 10^{5}$; (a) and (b)5s, (c) and (d) 30s, (e) and (f) 60 s

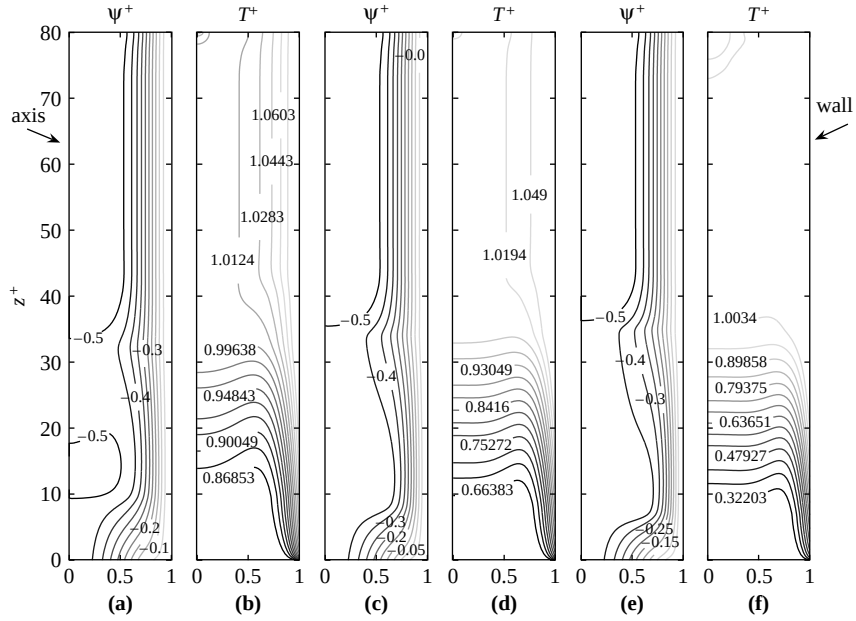

Figure 9.
Streamlines and isotherms along the pipe

Notes: For $t = 60$ s, $Re = 100$, $Gr = 2 \times 10^{5}$ and different ΔT^{+}; (a) and (b) −0.15, (c) and (d) −0.37, (e) and (f) −0.73

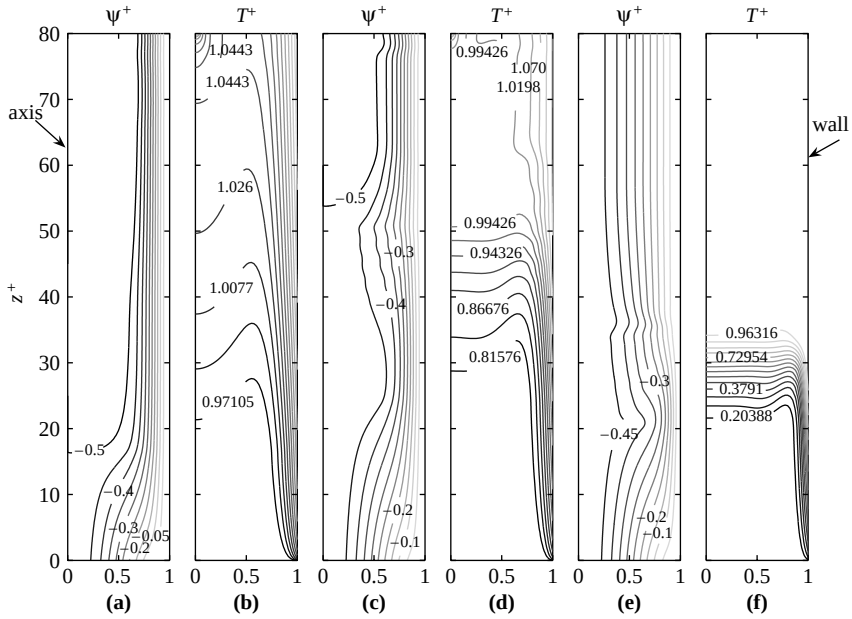

Figure 10.
Streamlines and isotherms along the pipe

Notes: For t = 30 s, Re = 300, $\Delta T^+ = -0.21$, $Gr = 7 \times 10^5$ and different a* ; (a) and (b) 100, (c) and (d) 70, (e) and (f) 40

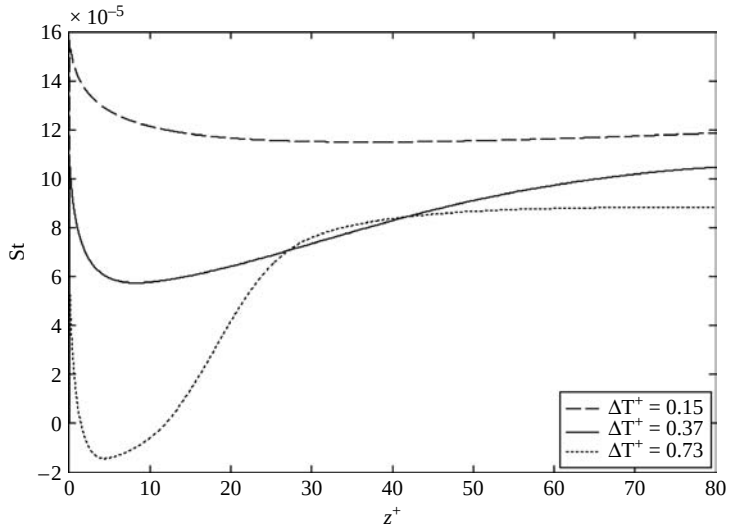

Figure 11.
Evolution of the Stanton number for different $\Delta T^+ > 0$

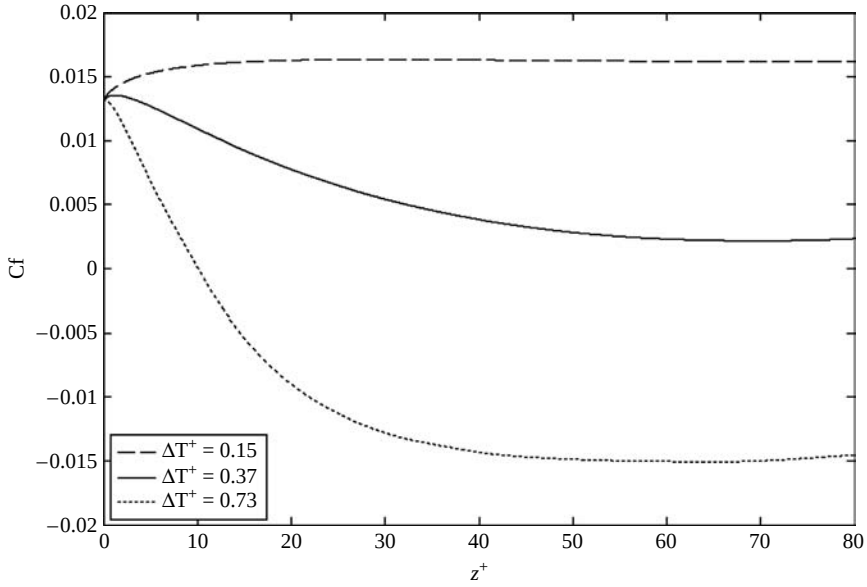

Figure 12.
Evolution of the friction factor for different $\Delta T^+ > 0$

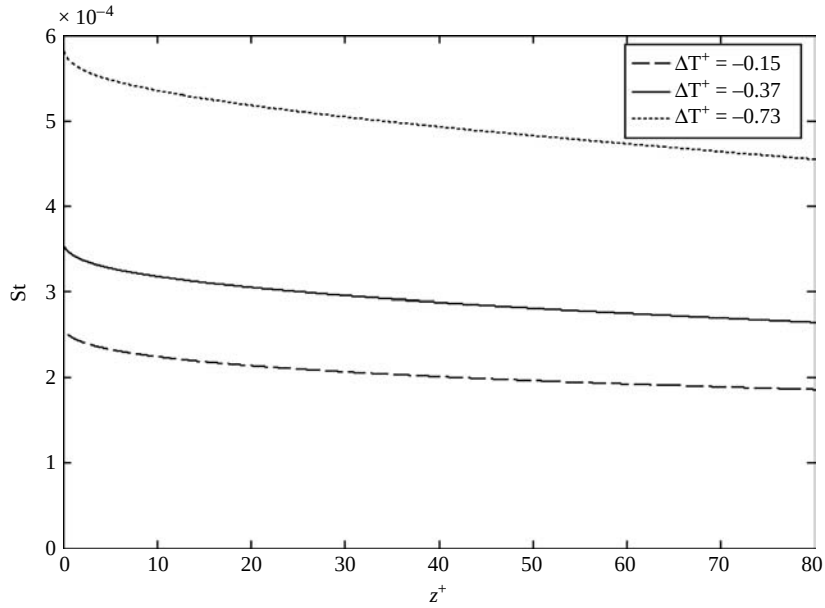

Figure 13.
Evolution of the Stanton number for different $\Delta T^+ < 0$

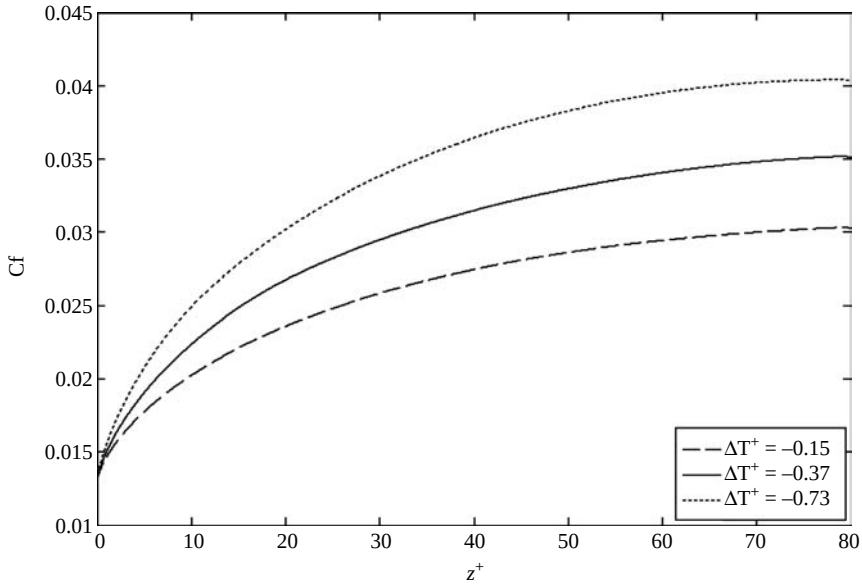

Figure 14.
Evolution of the friction factor for different $\Delta T^+ < 0$

at a relatively high ΔT^+. Moreover, the existence of a recirculating flow near the wall can lead to negative friction factor values.

In the cooling case, the reversal flow is produced in the central region of the pipe; it develops on top of the wave instability, and the flow becomes highly unstable for a high a^*. Both parameters, the Stanton number and the friction factor grow with the increasing of the temperature step.

Moreover, the analysis of the transient mixed convection in a vertical pipe allows to learn about the flow behaviour structures and consequently about the heat transfer of the fluid. This study should be very useful to improve heat transfer equipments.

References

Barletta, A. (2001), "Analysis of flow reversal for laminar mixed convection in a vertical rectangular duct with one or more isothermal walls", *Intern. J. Heat Mass Transfer*, Vol. 44, pp. 3481-97.

Behzamehr, A., Galanis, N. and Laneville, A. (2003), "Low Reynolds number mixed convection in vertical tubes with uniform wall heat flux", *Intern. J. Heat Mass Transfer*, Vol. 46, pp. 4823-33.

Bejan, A. (1984), *Convective Heat Transfer*, Chapter 12, Wiley, New York, NY.

Bernier, M.A. and Baliga, B.R. (1992a), "Visualization of upward mixed convection flows in vertical pipes using a thin semitransparent gold-film heater and dye injection", *Intern. J. Heat Fluid Flow*, Vol. 13, pp. 241-9.

Bernier, M.A. and Baliga, B.R. (1992b), "Conjugate conduction and laminar mixed convection in vertical pipes for upward flow and uniform wall heat flux", *Numerical Heat Transfer, Part. A*, Vol. 21, pp. 313-32.

Cheng, C.H., Kou, H.S. and Huang, W.H. (1990), "Flow reversal and heat transfer of fully developed mixed convection in vertical channels", *J. Thermophysics*, Vol. 4, pp. 375-83.

Gau, C., Yih, K.A. and Aung, W. (1992), "Reversed flow structure and heat transfer measurements for buoyancy-assisted convection a heated ducts, ASME", *J. Heat Transfer*, Vol. 111, pp. 928-35.

Hamadah, T.T. and Wirtz, R.A. (1991), "Analysis of laminar fully developed mixed convection in a vertical channel with opposing buoyancy", *ASME J. Heat Transfer*, Vol. 113, pp. 507-10.

Heggs, P.J., Ingham, D.B. and Keen, D.J. (1990), "The effects of heat conduction in the wall on the development of recirculating combined convection flows in vertical tubes", *Intern. J. Heat Mass Transfer*, Vol. 33, pp. 517-28.

Huang, T.M., Gau, C. and Aung, W. (1995), "Mixed convection flow and heat transfer in a heated vertical convergent channel", *Intern. J. Heat Mass Transfer*, Vol. 38, pp. 2445-56.

Joye, D.D. and Wojnovich, M.J. (1996), "Aiding and opposing mixed convection heat transfer in a vertical tube: loss of boundary condition at different Grashof numbers", *Intern. J. Heat Fluid Flow*, Vol. 17, pp. 468-73.

Kakac, S. and Yener, Y. (1995), *Convective Heat Transfer*, CRC Press, Boca Raton, FL.

Kakac, S., Li, W. and Cotta, R.M. (1990), "Unsteady laminar forced convection in ducts with periodic variation of inlet temperature", *J. Heat Transfer*, Vol. 112, pp. 913-20.

Lax, P.D. and Richtmyer, R.D. (1956), "Survey of the stability of linear finite difference equations", *Comm. Pure Appl Math*, Vol. 9, pp. 267-93.

Mai, T.H., Popa, C.V. and Polidori, G. (2005), "Transient mixed convection flow instabilities in a vertical pipe", *Heat Mass Transfer*, Vol. 41, pp. 216-25.

Morton, B.R., Ingham, D.B., Keen, D.J. and Heggs, P.J. (1989), "Recirculating combined convection in laminar pipe flow", *ASME J. Heat Transfer*, Vol. 111, pp. 106-13.

Nesreddine, H., Galanis, N. and Nguyen, C.T. (1998), "Effects of axial diffusion on laminar heat transfer with low Peclet numbers in the entrance region of thin vertical tube", *Numer Heat Transfer Part A*, Vol. 33, pp. 247-66.

Nguyen, C.T., EL Bécaye Maïga, S., Landry, M., Galanis, N. and Roy, G. (2004), "Numerical investigation of flow reversal and instability in mixed laminar vertical tube flow", *Intern. J. Thermal Sci*, Vol. 43, pp. 797-808.

Torrance, K.E. and Rockett, J.A. (1969), "Numerical study of natural convection in an enclosure with localized heating from below-creeping flow to the onset of laminar instability", *J. Fluid Mech*, Vol. 36, pp. 33-54.

Wang, M., Tsuji, T. and Nagano, Y. (1994), "Mixed convection with flow reversal in the thermal entrance region of horizontal and vertical pipes", *Intern. J. Heat Mass Transfer*, Vol. 37, pp. 2305-22319.

Zghal, M., Galanis, N. and Nguyen, C.T. (2001), "Developing mixed convection with aiding buoyancy in vertical tubes: a numerical investigation of different flow regimes", *Intern. J. Thermal Sci*, Vol. 40, pp. 816-24.

Corresponding author
Ton Hoang Mai can be contacted at: ton-hoang.mai@univ-reims.fr